Fibers and Polymers 2017, Vol.18, No.5, 907-914
DOI 10.1007/s12221-017-6899-z

ISSN 1229-9197 (print version)
ISSN 1875-0052 (electronic version)

Synthesis and Characterization of a Novel Charring Agent and Its Application in Intumescent Flame Retardant Polyethylene System

Mingwei Ba, Bing Liang*, and Changsong Wang

School of Material Science and Engineering, Shenyang University of Chemical Technology, Shenyang 110142, China

(Received September 15, 2016; Revised February 25, 2017; Accepted March 30, 2017)

Abstract: A novel charring agent poly(pentaerythritol spirocyclic phosphorusoxy spirocyclic diethanolamine borate) (PPSPSDB) was synthesized successfully with diethanolamine borate (DEAB) and spirocyclic pentaerythritol bisphosphorate disphosphoryl chloride (SPDPC), which was combined with ammonium polyphosphate (APP) to endow linear low-density polyethylene (LLDPE) with flame retardance. The structure of PPSPSDB was characterized by FTIR and ^{1}H-NMR. The study of thermal stability of various LLDPE composites showed that PPSPSDB/APP system could effectively improve the thermal degradation and thermal-oxidative stability of the char residues, and PE3 containing 30 wt% APP/ PPSPSDB with a 2 weight ratio left the highest amount of char residue at 800 ^{o}C. The results of flammability revealed that PE3 had the best combination property; the limited oxygen index value was 29.6, and vertical burning reached UL-94 V-0 rating, and the tensile strength and notched impact strength were 11.853 MPa and 28.8 kJ/m^2 respectively. The investigation of structure and morphology of char residue indicated that the compact foaming char layer, as a good barrier against the transmission of heat and volatiles, was formed for PE3 during combustion.

Keywords: Flame resistance, Synergistic effect, Intumescent flame retardant, Charring agent, Polyethylene composite

Introduction

Linear low-density polyethylene (LLDPE) is a commodity plastic, which is widely used in wire and cable, building pipe, film aspects because of its mechanical durability, good chemical resistance, low density, low toxicity, good electric insulation, and good processing ability, and so on [1,2]. LLDPE is a flammable polymer and its limiting oxygen index (LOI) value is about 17.5, therefore, the application of LLDPE has greatly been restricted [3]. In order to obtain good flame-retardant polyolefin composites, many flame retardants have been used in polyolefins, such as LLDPE and polypropylene. They include halogen-containing flame retardants (decarbomodiphenyl oxide and brominated epoxy), inorganic flame retardants (aluminum hydroxide (ATH) and magnesium hydroxide (MH)), and intumescent flame retardants (IFRs). As we all know, halogen-containing flame retardants are the most effective for improving the flame retardancy of polyolefins, especially when compounded with antimony trioxide [4-7]. Due to environmental safety concern, however, their uses have been severely limited in wire and cable aspects. Inorganic flame retardants and IFRs are the main halogen-free flame retardants applied in polyolefins. High loading of ATH and MH is needed to obtain the satisfying flame-retardant polyolefins. However, the high loading results in the dramatic decrease of mechanical properties and processing ability. Therefore, improving the flame resistance of LLDPE has become a recent focus of polymer research. Compared with inorganic flame retardants [8-12]. IFRs show much more effective flame retardancy in polyolefins, which have been studied and used more and more widely.

Among various means to improve the flame retardancy of LLDPE, the IFRs are of great interest and importance due to their environmental-friendliness and high char [13-17]. In the last decades, the ammonium polyphos-phate/pentaerythritol/ melamine (APP/PER/MA) system, a typical IFR, has been widely used. It is mainly composed of inorganic acid sources (e.g. ammonium polyphosphate, etc.), carbonifics (e.g. pentaerythritol, sorbitol, etc.) and spumifics (e.g. melamine, etc.) [18-20]. However, small-molecule MA and PER, having poor compatibility with the polymer matrix, easily migrate to the surface of the samples [21,22], thus resulting in a worsening of the flame retardancy. To surmount these deficiencies, many works have been turned to the seeking out the new charring agents.

To avoid the defect and to increase the char residue, a novel halogen-free phosphorus-nitrogen-boron-containing carbonization agent poly(pentaerythritol spirocyclic phosphorusoxy spirocyclic diethanolamine borate) (PPSPSDB), which shows high thermal stability because of the symmetrical structure and the incorporation of carbon abounding spirocyclic carbon, was synthesized by a polycondensation under high temperature successfully. The structure of PPSPSDB was characterized by fourier transform infrared (FTIR), ^{1}H-NMR. The thermal properties and flammability of intumescent flame retardant polyethylene (IFR-LLDPE) system using PPSPSDB as carbonization agent combining with APP were investigated. The thermal and combustion behaviors of various LLDPE compounds were investigated by thermogravimetric analysis (TGA), limiting oxygen index (LOI) and UL-94 test. The structure

*Corresponding author: lb1007@163.com

and morphology of char residues were studied by FTIR and scanning electronmicroscopy (SEM). The mechanical properties were also investigated.

Experimental

Materials

All of the starting materials and solvents were commercially available and were used without further purification. Linear low density polyethylene (LLDPE) was provided by Petro China Co Ltd. (Liaoning, China); APP was provided by Changfeng Chemical Corp. (Shifang, China). Pentaerythritol (PER), toluene, tetrahydrofuran, diethanolamine, boric acid, chlorobenzene, N,N-Dimethylformamide (DMF) and dichloromethane (CH_2Cl_2; analytical reagent (AR)) were purchased from Sinopharm Chemical Reagent (Liaoning, China). Phosphorus oxychloride ($POCl_3$, AR) was purchased from Beijing Lideshi Chemical Co. Ltd. (China).

Synthesis of DEAB

A 250 m*l* three-necked round bottom flask equipped with a magnetic stirrer, reflux condenser, thermometer and water knockout vessel were placed into a oil bath. 24.7 g (0.4 mol) boric acid, 92.5 g (0.88 mol) diethanolamine and 100 m*l* toluene were added and stirred at 110 °C until no water were generated in the reaction system. Then, the reaction mixture was cooled to room temperature slowly, toluene was removed by vacuum distillation and a pale yellow viscous liquid was obtained. Finally, the yellow liquid was refined by washing with tetrahydrofuran (THF) repeatedly. After the refined product was dried at 50 °C in vacuum for 12 hrs, a white liquid was obtained and named as diethanolamine borate (DEAB). The yield of the DEAB product was 85.3 %. The whole reaction equation is illustrated in Scheme 1.

Synthesis of SPDPC

A 250 m*l* three-necked round bottom glass equipped with a temperature controller, a magnetic strirrer and a reflux condenser were 32.6 m*l* (0.35 mol) of phosphorus oxychloride, 17.7 g of pentaerythritol, 0.1 g of DMAP and 100 m*l* of chlorobenzene. The temperature of the reaction mixture was raised to 60 °C and maintained for 2 hrs under a nitrogen gas atmosphere. Afterwards, the reaction mixture was heated slowly to 100 °C and maintained for 10 hrs. After cooling to room temperature, the precipitate was filtered and washed with dichloromethane (CH_2Cl_2). After the refined product was dried at 80 °C in vacuum for 12 hrs, a white solid powder was obtained (yield: 88 %). The whole reaction equation is illustrated in Scheme 2.

Synthesis of PPSPSDB

A 250 m*l* three-necked round bottom flask equipped with a magnetic stirrer, reflux condenser, thermometer and vacuum distillation unit were placed into an oil bath. 26.2 g (0.12 mol) DEAB, 29.7 g (0.1 mol) SPDPC and 100 m*l* DMF were added and stirred at 120 °C for 2 hrs, before the solvent was distilled off under reduced pressure and the temperature was raised to 190 °C for 2 hrs. Then, the reaction mixture was cooled to room temperature slowly, a crisp bright yellow solid was obtained. Finally, the milled solid was filtered and washed with DMF repeatedly. After the

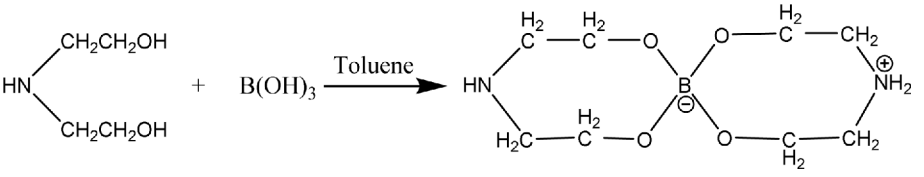

Scheme 1. Synthesis route of DEAB.

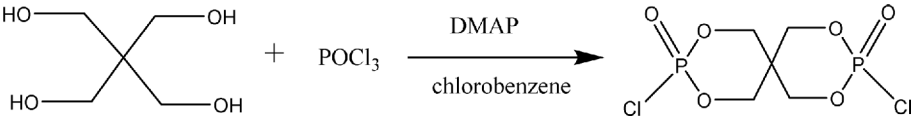

Scheme 2. Synthesis route of SPDPC.

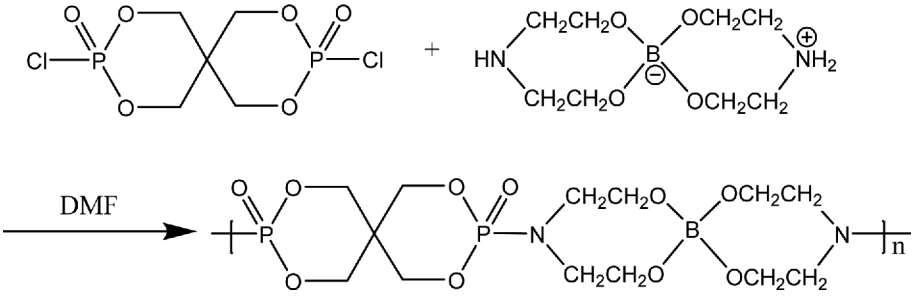

Scheme 3. Synthesis route of PPSPSDB.

refined product was dried at 60 °C in vacuum for 6 hrs, a bright yellow solid powder was obtained. The yield of the PPSPSDB product was 83.6 %. The whole reaction equation is illustrated in Scheme 3.

Preparation of Flame Retarded LLDPE Compounds

The samples were prepared on a torque rheometer with the roll speed of 50 rpm at 170 °C. APP/PPSPSDB (30 wt%) with different ratios were added into LLDPE matrix and the formulations of prepared samples are presented in Table 1. PPSPSDB and APP with the desired amount were added into melting LLDPE for about 10 min. After the composites were mixed uniformly, the composite samples were hot pressed under 10 MPa at 170 °C for 5 min and cold pressed under 10 MPa at room temperature for 3 min, then cooled to room temperature. The specimens were prepared finally.

Characterization

FTIR (NICOLET 470) was used to characterize the chemical structure of DEAB, SPDPC and PPSPSDB.

The ^{1}H-NMR was performed on a Bruker Avance 500 MHz spectrometer by using DMSO as solvent and $CDCl_3$ as a reference respectively.

Thermogravimetric analyzer (STA 449C) was used, and the test temperature ranged from ambient to 800 °C at a heating rate of 10 °C min^{-1} under nitrogen, and the sample's weight was about 10 mg in each test.

Scanning electron microscopy (SEM JSM-6360LV) was used to investigate the char surface of flame-retardant LLDPE. The surface of char residues was clad with gold before SEM scanning, and the char residues were obtained from the burned samples in the vertical burning test.

Oxygen index instrument (JF-3) was used to measure the limited oxygen index (LOI) of samples with the dimensions of 130×6.5×3 mm^3 according to ASTM D2863-97.

The vertical burning tests (UL-94) were performed in CZF-3 horizontal and vertical burning test instrument with sample dimension of 130×13×3 mm^3 according to ASTM D3801. The tensile and impact behavior tests were carried out in TCS-2000 tensile test equipment and GT-7045-MDL digital impact tester according to ASTM D638 and ASTM D256, respectively, and the listed data were the mean of five samples.

Table 1. Formulations of various LLDPE compounds

Sample	LLDPE (wt%)	APP (wt%)	PPSPSDB (wt%)	LOI (%)	UL-94
PE0	100	-	-	17.4	Burning
PE1	70	30	-	23.1	V-2
PE2	70	22.5	7.5	28.8	V-0
PE3	70	20	10	29.6	V-0
PE4	70	15	15	26.5	V-0
PE5	70	-	30	23.6	V-2

Results and Discussion

Characterization of DEAB, SPDPC and PPSPSDB

FTIR and ^{1}H-NMR Characterization of DEAB

The structure of DEAB was characterized by FTIR and shown in Figure 1. The peaks at 3400 and 1646 cm^{-1} corresponded to the stretching vibration and bending vibration of -NH, respectively. The stretching vibration of -CH_2 is observed at 2909 and 2862 cm^{-1}. The peak at 1461 cm^{-1} is assigned to -CH bending vibration. Furthermore, the peak at 867 cm^{-1} is the characteristic absorption peak of the B-O bond.

The structure of DEAB is characterized by ^{1}H-NMR spectrum and illustrated in Figure 2. The peak at 3.38 and 3.89 ppm are assigned to the proton of -NH and -NH_2, respectively. The peak at 3.68 ppm is associated with -CH_2 protons near the spirocyclic boron. The peak at 2.75 ppm is assigned to the proton of -CH_2 out of the spirocyclic boron. The peak at 7.24 ppm comes from the solvent. These results confirm that the chemical reaction takes place as in Scheme 1.

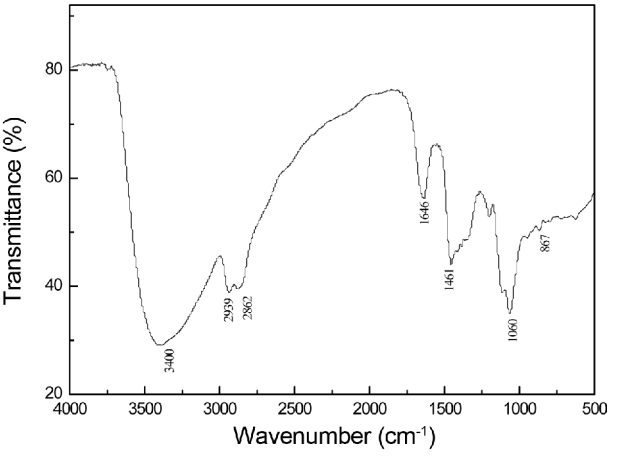

Figure 1. FTIR spectrum of DEAB.

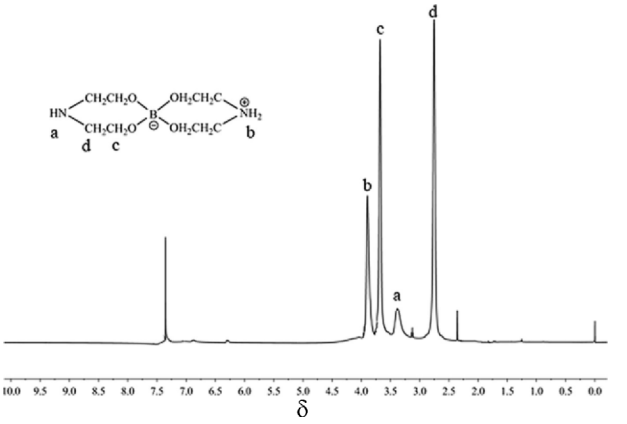

Figure 2. ^{1}H-NMR spectrum of DEAB.

FTIR and ^{1}H-NMR Characterization of SPDPC

SPDPC was characterized by FTIR (Figure 3). In detail, the peaks at 1308 cm^{-1} and 1027 cm^{-1} were associated with the stretching mode of P=O and P-O-C in the phosphate, respectively. The absorption bands of P-O stretching at nearly 854 cm^{-1}. The stretching vibration of P-Cl is observed at 549 cm^{-1}.

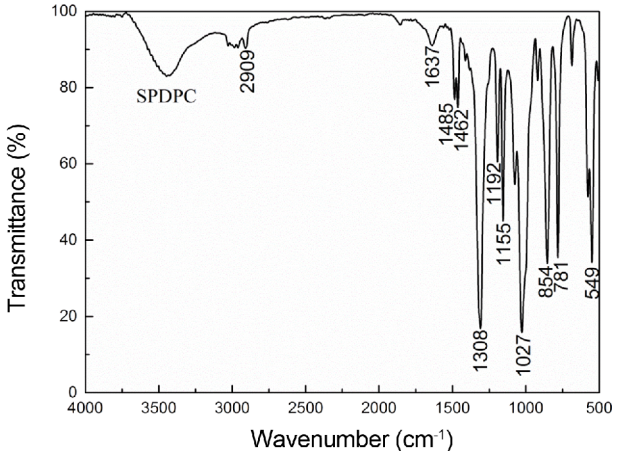

Figure 3. FTIR spectrum of SPDPC.

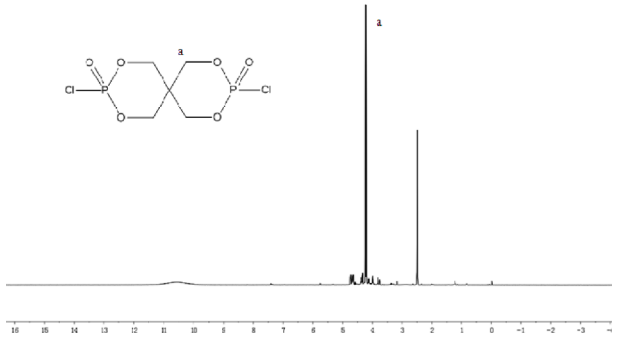

Figure 4. ^{1}H-NMR spectrum of SPDPC.

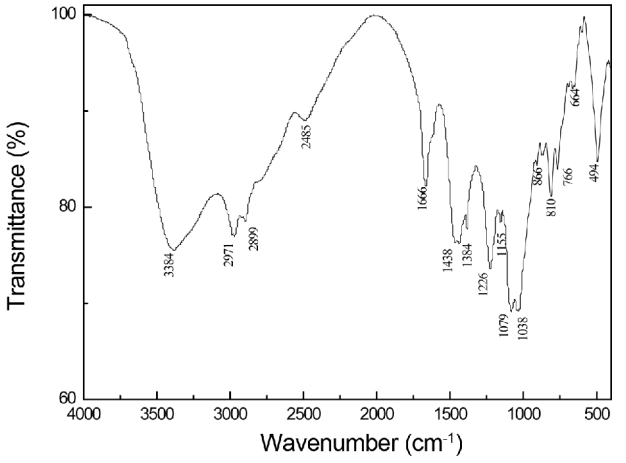

Figure 5. FTIR spectrum of PPSPSDB.

The ^{1}H-NMR spectrum of SPDPC is shown in Figure 4. The peak at 4.19 ppm is associated with -CH_2 (a) protons adjacent to the spirocyclic carbon. The peaks at 2.49 ppm belong to protons of the DMSO solvent. The chemical shifts of the absorption peaks and the area ratios of the peak integration are identical to the expected chemical structure.

FTIR, ^{1}H-NMR and TGA Characterization of PPSPSDB

The structure of PPSPSDB was characterized by FTIR and is illustrated in Figure 5. The stretching vibration of -NH is observed at 3384 cm^{-1}. The absorption at 2971 and 2899 cm^{-1} is assigned to the stretching vibration of -CH_2. The peak at 1384 cm^{-1} is associated with the stretching vibration of -CN. The peak at 866 cm^{-1} is the characteristic absorption peak of the B-O bond. The absorption peak of P=O is observed at 1226 cm^{-1}.The peaks at 1079 cm^{-1} and 810 cm^{-1} were associated with the stretching mode of P-O-C and P-O, respectively. Moreover, the peak of 1038 cm^{-1} is associated with the stretching vibration of P-N, the characteristic band of P-Cl disappears at 549 cm^{-1}. It indicates that the final product was obtained successfully.

The ^{1}H-NMR spectrum of PPSPSDB is shown in Figure 6. The signal at 3.65 ppm is attributed to the -CH_2 (c) protons adjacent to the spirocyclic boron. The peak of -CH_2 (b) protons out of the spirocyclic boron is observed at

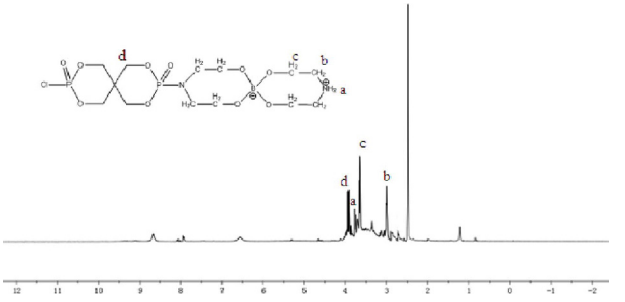

Figure 6. ^{1}H-NMR spectrum of PPSPSDB.

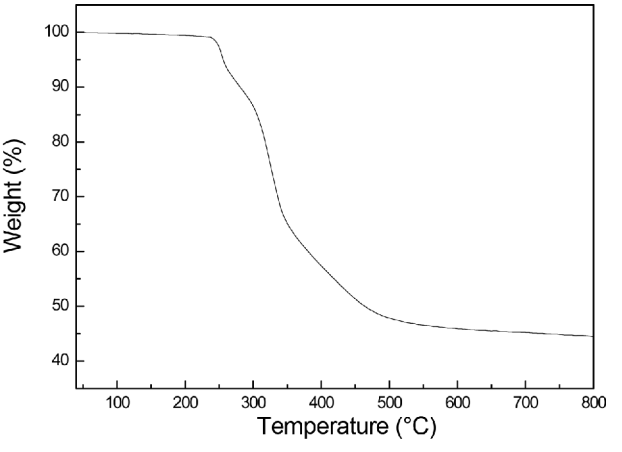

Figure 7. TGA curve of PPSPSDB under nitrogen atmosphere.

2.98 ppm. The peak at 3.91 ppm is associated with -CH_2 (d) protons adjacent to the spirocyclic carbon. The peak at 3.81 ppm is associated with P-NH (a), which confirms the final structure of PPSPSDB. The peaks at 2.48 ppm belong to protons of the DMSO solvent. The chemical shifts of the absorption peaks and the area ratios of the peak integration are identical to the expected chemical structure.

The TGA curve of PPSPSDB in nitrogen atmosphere is shown in Figure 7. PPSPSDB presents a two-step decomposition in the temperature ranges of 250-350 °C and 350-800 °C, corresponding to the loss of water and small molecules such as NH_3, the further carbonization and the thermal degradation of char residue, respectively. Besides, the char residue of PPSPSDB at 800 °C is 44.45 %, implying the high charring ability.

Flammability

This novel PPSPSDB which was synthesized in our work was mixed with APP and LLDPE to obtain a new IFR system. To evaluate the flame retardancy properties and the synergy of the two components, the LOI and vertical burning test (UL-94) were conducted. LOI and UL-94 are widely used to evaluate the flame resistance of polymer composites. LOI is defined as the minimum. The sample can be considered as a flame-retardant material when the LOI value is more than 26. UL-94 test results fall into three categories, with burning ratings V-0, V-1 and V-2, and the V-0 rating corresponds to the highest level of flame resistance. The results are given in Table 1.

The LOI values and the UL-94 results of various samples are given in Table 1. Pure LLDPE is highly combustible with molten drips, the LOI value is only 17.4 and UL-94 cannot reach any rating. Compared with pure LLDPE, LLDPE/APP and LLDPE/PPSPSDB/APP, the LLDPE/PPSPSDB/APP composites show a better flame resistance performance. The LOI values of LLDPE/APP (PE1) and LLDPE/PPSPSDB (PE5) with 30 wt% loadings are 23.1 and 23.6, respectively, and neither can reach UL-94 V-0 rating. Flame retardancy of PPSPSDB was little better than that of APP in LLDPE systems. This demonstrated that APP and PPSPSDB alone showed low efficiency in flame retardancy of LLDPE. When PPSPSDB and APP were mixed in a certain proportion, LOI values of IFR-LLDPE systems were remarkably enhanced and approached 30. For LLDPE/PPSPSDB/APP systems, the LLDPE samples exhibit a remarkable increase in LOI and reach V-0 rating in UL-94. The best ratio of APP and PPSPSDB (PE3) is 2 which LOI is 29.6, the increment of LOI (ΔLOI) is 12.2 when compared with pure LLDPE, and the UL-94 V-0 rating can be achieved. When the APP was added into the PPSPSDB, because the synergistic effect improved the performance of the flame, Moreover, no dripping was observed during UL-94 test, so the char-forming agent PPSPSDB shows an excellent antidripping property.

The reason may be that with the effective charring agent (PPSPSDB), the char can be rapidly formed as encountering fire or heat, and change the viscosity of the melting matrix, which impedes the flame propagation and protects the matrices from combustion. In addition to, the reason for PPSPSDB's better flame resistance is attributed to the combination of P, N and B elements and the special molecular structure [23]. When LLDPE/PPSPSDB/APP systems burns at a lower temperature, the P=O bonds provide the acid resource, the rigid spirocyclic groups connecting P=O play an anti-burning effect to a certain extent, the N element would turn into incombustible NH_3 and the B element will be changed into B_2O_3 or boric acid. Meanwhile, volatile gases like NH_3 and H_2O derived from the decomposition of APP were produced. Both the formation of the condensed phase and the release of gas phase led to the appearance of an original intumescent char layer consist of B-O, P-N, P=O and P-O-P etc. structures. Then, with further increasing the temperature, APP decomposed to produce phosphoric acid, polyphosphoric acid, and metaphosphoric acid, which could delay the fracture of spiro groups and make more spiro rings evolve into the char layer. The enrichment of the condensed phase promoted the formation of an integrated, compact and stable char layer, resulting in the excellent flame retardancy of LLDPE/PPSPSDB/APP composite.

Thermal Stability

Thermogravimetric analysis (TGA) is a common technique for evaluating the thermal stability of various polymers, and it also indicates the decomposition behaviors of the polymer at various temperatures [24,25]. Thermal degradation behavior of different LLDPE samples in nitrogen atmosphere is investigated by TGA and DTG, as shown in Figure 8. The onset decomposition temperature (Td) is defined as the temperature of 5 % weight loss. The relative thermal stability of the samples is evaluated by Td and the char yield at 800 °C, which are listed in Table 2.

As the samples are easy to absorb moisture, a small amount of water infiltrated into the samples caused a small amount of weight loss behavior bellow 100 °C. Pure LLDPE exhibits to one step decomposition in the range of 420-490 °C, mainly ascribed to the degradation of polyethylene backbone. When the temperature is higher than 500 °C, the weight will not decrease any longer and the char residue is negligible. The Td for the pure LLDPE is about 449 °C. The addition of 30 wt% PPSPSDB into LLDPE improves the thermal stability above 480 °C and increases the char residue to 15.06 % at 800 °C but worsens its tolerance of the heat shock below 480 °C due to the early degradation of PPSPSDB. The Td for the APP is about 330 °C, and the char residue of APP at 800 °C is 15.07 %. In contrast, the 30 wt% APP addition can not only postpone the decomposition of LLDPE backbone but also from 12.46 % remains at 800 °C (Table 2), which will certainly be attributed to the protective effect

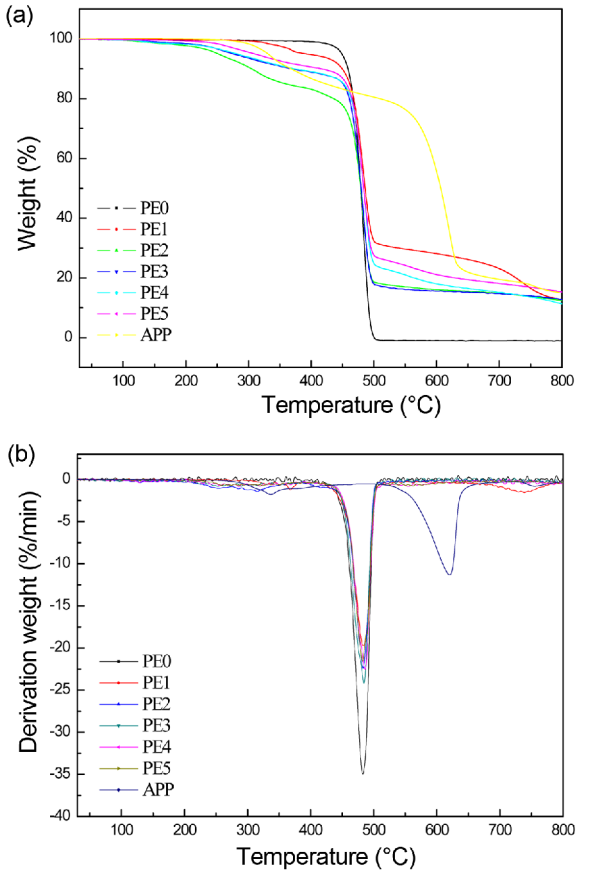

Figure 8. TGA (a) and DTG (b) curves of LLDPE samples in nitrogen atmosphere.

Table 2. TGA data of various LLDPE samples in nitrogen atmosphere

Sample	$T_{5\%}$ (°C)	Char residue at 800 °C (%)
PE0	449	0
PE1	391	12.46
PE2	251	12.19
PE3	275	12.81
PE4	281	11.05
PE5	309	15.06
APP	330	15.07

of the degraded products of APP like polyphosphoric acid and polymetaphosphate. When it comes to the combination of APP with PPSPSDB, PE3 shows the improved thermal stability and the most char residue of 12.81 % among all the samples at 800 °C, which is closely associated with the positive synergistic effect between APP and PPSPSDB when the weight ratio of APP to PPSPSDB is 2 in the matrix. These results indicate that the optimum weight ratio of acid source, carbonization agent and blowing agent is crucial for the formation of the best protective char layer.

Characterization of Char Residue of Various LLDPE Composites

The intumescent flame retardant systems always endure an expansion and the formation of the char layer; thus, the investigation of the differences of char residues after combustion is necessary. The microstructure of the char

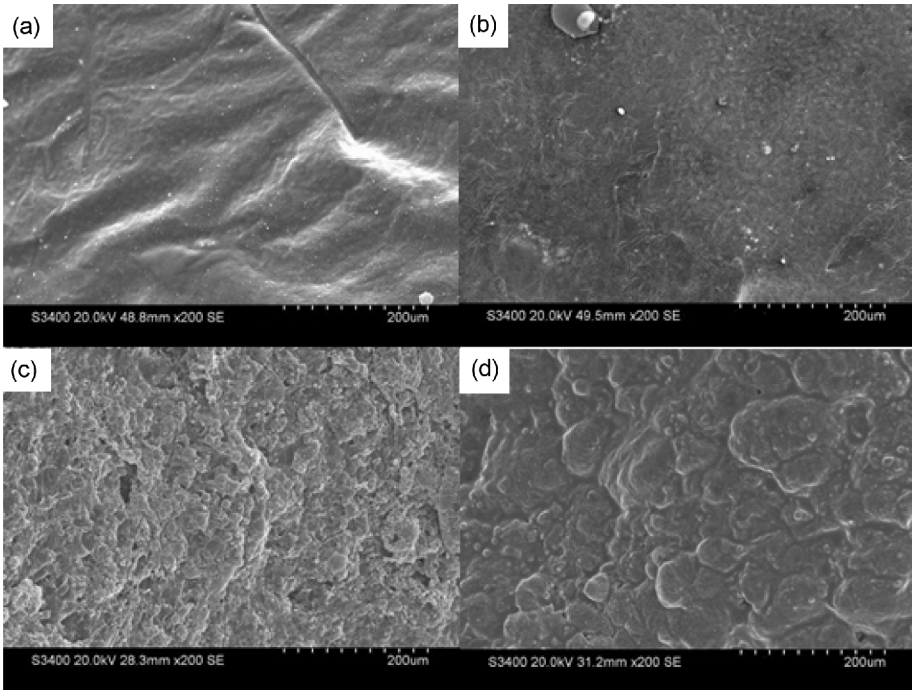

Figure 9. SEM images of the char residues of (a) PE0, (b) PE1, (c) PE3, and (d) PE5.

residues after combustion was investigated using SEM. The morphologies of the char residues are shown in Figure 9.

Pure LLDPE leaves nothing, and just a tiny residue of PE1 with 30 wt% APP is observed. The residue is intensely discontinuous and absent of any intumescences. In contrast, PE3 with a weight ratio of APP to PPSPSDB being 2 engender a compact and continuous intumescent char residues. The explanation that the forming bubbles during the combustion broke to release the inner pressure of the char, thus leading to the appearance of various folds in its cooling process, whereas PE3 containing the appropriate amount of PPSPSDB produces the most optimum char layer; that is, there are many tiny bubbles embedded on the surface of each large bubble. These together endow its char layer with good barrier against the transmission of heat and volatiles. In contrast, the char layers of PE5 are some large protruding structures on the smooth char layer surface, which probably explained why these char-layers are low efficient and poor thermal stability. These results indicate that PE3 has the best intumescent char layer as a physical barrier against the transfer of the heat and combustible gases, thus resulting in highest char residue at 800 ^{o}C.

Mechanical Properties

The results show that the LLDPE/PPSPSDB/APP composites lower tensile and impact strengths than pure LLDPE, which are listed in Table 3. When the best ratio of APP and PPSPSDB (PE3) is 2, the tensile and impact strengths of the flame-retarded sample PE3 were decrease to 27.8 % and 29.1 % for pure LLDPE, respectively. Amhmad *et al.* [26], added 30 wt% of ATH to the polyolefin, the LOI was 22.5, the tensile and impact strengths of the polyolefin-30 wt% ATH was decrease to 35.5 % and 62.6 % for pure polyolefin, respectively. In contrast, the mechanical properties of the LLDPE/PPSPSDB/APP composites were less affected. The dispersion of the FR-LLDPE samples was investigated using SEM (Figure 10). In Figure 10, APP and PPSPSDB could relatively uniformly distribute in LLDPE. The results show that the main reason for the diminished mechanical strength was the poor dispersion of PPSPSDB and APP in the LLDPE matrix. Furthermore, PPSPSDB had a rigid molecular structure with higher phosphorus, N_2 contents and boron spiro. The rigid structure produces steric hindrance, which decreases the cross-linking density of LLDPE; therefore, the mechanical properties of the flame-retarded LLDPE compounds undergo clear deterioration.

Table 3. Mechanical properties of various LLDPE compounds

Sample	Tensile strength (MPa)	Impact strength (kJ/m^2)
PE0	16.5	40.6
PE1	9.3	16.3
PE2	10.2	23.2
PE3	11.9	28.8
PE4	10.6	25.9
PE5	9.1	15.9

Conclusion

A novel charring agent PPSPSDB was synthesized successfully with DEAB and SPDPC, and its chemical structure was characterized by FTIR and ^{1}H-NMR. PPSPSDB was combined with APP to fabricate flame retardant LLDPE compounds. The thermal stability was studied by TGA, and the results showed that PPSPSDB/APP system could be effective to improve the thermal degradation and thermal-oxidative stability of the char residues and PE3 with 2 weight ratio of APP to PPSPSDB presented the highest thermal stability. Their flammability was investigated via LOI test and UL-94, the LOI value of PE3 reaches 29.6 and the results revealed that PE3 had the highest flame retardancy. The PPSPSDB integrated the P, N and B elements and it shows a good ability of char formation itself. The char residue of PPSPSDB could reach 44.45 wt% at 800 ^{o}C. Moreover, the study of morphology of char residue by SEM indicated that PE3 formed the best char layer during the combustion, which effectively protected the inner char layer from the flame. The results also show that the tensile strength and impact strength of sample were 11.853 MPa and 28.8 kJ/m^2. PPSPSDB is not only used in intumescent flame retardant systems of LLDPE to obtain good flame

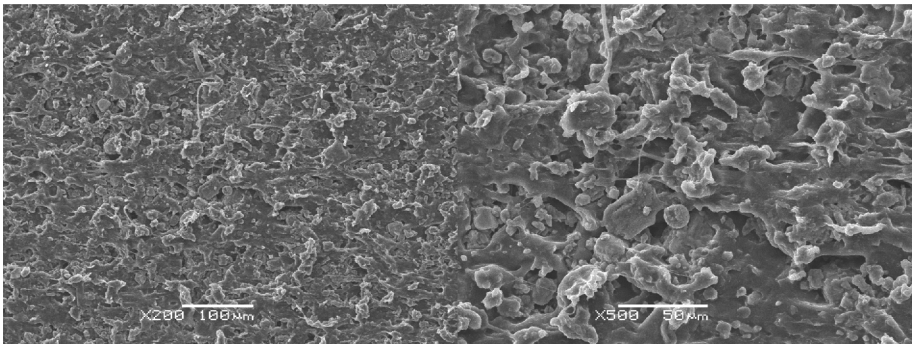

Figure 10. SEM images of the dispersion of the FR-LLDPE samples.

retardancy, but also the effect of it on mechanical properties is low, compared with pure LLDPE system. As a novel charring agent, PPSPSDB has the potential to be industrialized in the near future.

Acknowledgements

The National Science-technology Support Plan, China (agreement code: 2012BAB06B03), the Liaoning Provincial Science and Technology Program, China (agreement code: 2015304002) and the International Technical Cooperation and Exchanges Specific Funds, China (agreement code: 2013DFA51200).

References

1. F. Xie, Y. Z. Wang, B. Yang, and Y. Liu, *Macromol. Mater. Eng.*, **291**, 247 (2006).
2. D. Y. Wang, Y. Liu, Y. Z. Wang, C. P. Artiles, T. R. Hull, and D. Price, *Polym. Degrad. Stabil.*, **92**, 1592 (2007).
3. J. Green in "Flame Retardant Polymeric Material" (M. Lewin, S. M. Atlas, and E. M. Pearce Eds.), Vol. 3, Plenum Press, New York, 1982.
4. N. Wu and R. J. Yang, *Polym. Adv. Technol.*, **22**, 495 (2011).
5. J. Q. Huang, Y. Q. Zhang, Q. Yang, X. Liao, and G. X. Li, *J. Appl. Polym. Sci.*, **123**, 1636 (2012).
6. Q. B. Zhang, H. T. Xing, C. Y. Sun, H. W. Xiang, and D. W. Jiang, *J. Appl. Polym. Sci.*, **115**, 2170 (2009).
7. D. Y. Wang, X. X. Cai, M. H. Qu, Y. Liu, and J. S. Wang, *Polym. Degrad. Stabil.*, **93**, 2186 (2008).
8. K. Wun, Z. Z. Wang, and H. J. Liang, *Polym. Compos.*, **29**, 854 (2008).
9. L. Hendrickson and K. B. Connole, *Polym. Eng. Sci.*, **35**, 211 (1995).
10. Y. Liu, Z. Q. Feng, and Q. Wang, *Polym. Compos.*, **30**, 221 (2009).
11. Y. Liu and Q. Wang, *Polym. Compos.*, **28**, 163 (2007).
12. J. C. Wang and Y. H. Chen, *J. Elastomers. Plast.*, **39**, 33 (2007).
13. S. Bourbigot, M. Lebras, S. Duquesne, and M. Rochery, *Macromol. Mater. Eng.*, **289**, 499 (2004).
14. G. Camino, L. Costa, L. Trossarelli, F. Costanzi, and A. Pagliari, *Polym. Degrad. Stabil.*, **12**, 213 (1985).
15. K. K. Baljinder and A. R. Horrocks, *Polym. Degrad. Stabil.*, **54**, 289 (1996).
16. G. Sabyasachi, S. Gang, H. Katherine, and H. E. Mark, *Polym. Degrad. Stabil.*, **93**, 99 (2008).
17. S. H. Chiu and W. K. Wang, *Polymer*, **39**, 1951 (1998).
18. B. Li and X. C. Zhang, *Chem. J. Chin. Univ.*, **20**, 146 (1999).
19. B. Youssef, B. Mortaigne, M. Soulard, and J. M. Saiter, *J. Therm. Anal. Calorim.*, **90**, 489 (2007).
20. M. Lewin and M. Endo, *Polym. Adv. Technol.*, **14**, 3 (2003).
21. Y. H. Chen, Y. Liu, Q. Wang, and R. Kierkels, *Polym. Degrad. Stabil.*, **81**, 215 (2003).
22. Q. Wang, Y. H. Chen, Y. Liu, H. Yin, and N. Aelmans, *Polym. Int.*, **53**, 439 (2004).
23. B. Liang, X. D. Hong, M. Zhu, and C. J. Gao, *Polym. Bull.*, **72**, 2967 (2015).
24. D. Q. Chen, Y. Z. Wang, X. P. Hu, and D. Y. Wang, *Polym. Degrad. Stabil.*, **88**, 349 (2005).
25. H. Ren, J. Z. Sun, B. J. Wu, and Q. Y. Zhou, *Polym. Degrad. Stabil.*, **92**, 956 (2007).
26. S. A. A. Ramazani, A. Rahimi, M. Frounchi, and S. Radman, *Mater. Des.,* **29**, 1051 (2008).